Stepwise Approach to Bimetalic Porphyrin Hosts: Spatially Enforced Coordination of a Nickel(II) Porphyrin

Anton Vidal-Ferran, Nick Bampos, and Jeremy K. M. Sanders*

Cambridge Centre for Molecular Recognition, University Chemical Laboratory, Lensfield Road, Cambridge CB2 1EW, U.K.

Received September 26, 1997[⊗]

The synthesis of the Zn_3 1,1,2-trimer **$Zn_3$3** and the $NiZn_2$ 1,1,2-trimer **$NiZn_2$3** by a stepwise convergent route is described. A large affinity for **Py_3T** by both cyclic 1,1,2-trimers, **$Zn_3$3** or **$NiZn_2$3**, with respect to the linear trimers, provides a thermodynamic driving force for the templated cyclization of the new host molecules, which were fully characterized by NMR spectroscopy (COSY and NOESY). The binding properties of several pyridine-containing bidentate and tridentate ligands have been investigated in order to probe the shape and the size of the cavity of the host molecule. Both **Py_2Pr** and **Py_2Py** bind very strongly to **$Zn_3$3** and **$NiZn_2$3** (ligand affinities in CH_2Cl_2 at 25 °C, $>10^8$ M^{-1}), while the tridentate ligand **Py_3T** binds to both **$Zn_3$3** and **$NiZn_2$3** with a very high binding constant (ligand affinities in CH_2Cl_2 at 25 °C, $>10^9$ M^{-1}). This unexpected result for **$NiZn_2$3** suggests that the cavity-enforced effective molarity of the third pyridyl of **Py_3T** at the Ni site is high enough to form the first example of a stable 1:1 Ni(II)−pyridyl complex. The resulting Ni(II) paramagnetic complex has been characterized by NMR; the temperature dependence deviates slightly from ideal Curie behavior.

Introduction

One of the key aims of supramolecular chemistry is to create enzyme mimics capable of recognition and catalysis. The first major milestone of our research in this area was the controlled synthesis of the 2,2,2-trimer **$Zn_3$1** (Chart 1) and related dimers and trimers using templated Glaser−Hay coupling of preformed porphyrin monomers.[1,2] To aid discussion and comparison of these closely-related analogues, we introduce a shorthand notation for the number of ethyne links between building blocks. Thus, the original butadiyne-linked trimer **$Zn_3$1** is denoted 2,2,2, while **$Zn_3$2** (Chart 1), is the 1,1,1-cyclic trimer. It was an important part of our strategy that we should create a series of receptors of the same shape but with a range of cavity sizes using diarylporphyrin monomers as the building blocks. We have previously described a "stretched" 4,4,4-trimer[3] and a platinum-linked analogue,[4] each of which possesses a cavity larger than that of **$Zn_3$1**. The 2,2,2-trimer has proved to be a versatile object for molecular recognition, stereoselectively accelerating an *exo*-Diels−Alder reaction,[5] and also catalyzing zinc porphyrin acyl transfers.[6] However, synthesis of oligomers from monomers by the Glaser−Hay route severely limits the range of architectures and the cavity size which can be prepared. In order to synthesize oligomers with a smaller cavity, a statistical approach utilizing preformed dialdehyde units has been developed.[7] The synthetic strategy requires a multiple porphyrin unit synthesis, after which multimilligram quantities of cyclic 1,1-dimer and cyclic 1,1,1-trimer **$Zn_3$2** are obtained. However, the combination of low yield and difficulty in separation of **$Zn_3$2** from higher oligomers renders this route less attractive for providing large quantities of 1,1,1-trimer.[7] This paper reports a versatile general route to the 1,1,2 system, exemplified by **$Zn_3$3** (Chart 1) and **$NiZn_2$2**, and some unusual properties.

Our efforts have concentrated on the preparation of zinc porphyrin hosts because they exhibit a number of advantages over other metals: they are diamagnetic and can be readily studied spectroscopically by NMR, can easily be prepared from free-base porphyrins, can be readily demetalated with dilute acid, and form five-coordinate 1:1 complexes with amine ligands which have suitable binding constants for measurement by NMR or UV/vis titration. Recently, the range of building blocks has been expanded to include the d^6 ruthenium carbonyl porphyrin monomer **Ru4**, which has been used in the stereospecific templated synthesis of the 2,2,2-trimer **$Ru_3$1**.[8]

Driven by the desire to control and direct binding inside the cavity, we envisaged a synthetic strategy which provides porphyrin oligomers with two different metalic species. The new route, which is summarized in Scheme 1, would lead to a monoethyne-linked linear trimer which contains a unique metaloporphyrin core linked to two identical metaloporphyrin units. The resulting host will be smaller than the original 2,2,2-trimer and preserve, if not enhance, the recognition and catalytic properties exhibited by the original butadiyne-linked trimer. Furthermore, should the (unique) porphyrin core bind nitrogen-containing ligands weakly (by appropriate choice of metal), binding inside the host will then be dictated by the two available zinc sites, the binding properties of which are well understood. A receptor with this property will provide fresh insight into the *exo*-Diels−Alder and acyl transfer processes catalyzed by the original 2,2,2-trimer. Nickel(II) seemed a suitable candidate

* To whom correspondence should be addressed. E-mail: jkms@cam.ac.uk.
⊗ Abstract published in *Advance ACS Abstracts,* December 1, 1997.

(1) Sanders, J. K. M. In *Comprehensive Supramolecular Chemistry*; Atwood, J. L., Davies, J. E. D., MacNicol, D. D., Vögtle, F., Eds.; Elsevier: Amsterdam, 1996; Vol. 9, pp 131−164.
(2) (a) Anderson, S.; Anderson, H. L.; Sanders, J. K. M. *Acc. Chem. Res.* **1993**, *26*, 469. (b) Anderson, S.; Anderson, H. L.; Sanders, J. K. M. *J. Chem. Soc., Perkin Trans. 1* **1995**, 2247.
(3) Anderson, H. L.; Walter, C. J.; Vidal-Ferran, A.; Hay, R. A.; Lowden, P. A.; Sanders, J. K. M. *J. Chem. Soc., Perkin Trans. 1* **1995**, 2275.
(4) Mackay, L. G.; Anderson, H. L.; Sanders, J. K. M. *J. Chem. Soc., Perkin Trans. 1* **1995**, 2269.
(5) (a) Bonar-Law, R. P.; Mackay, L. G.; Walter, C. J.; Marvaud, V.; Sanders, J. K. M. *Pure Appl. Chem.* **1994**, *66*, 803. (b) Walter, C. J.; Sanders, J. K. M. *Angew. Chem., Int. Ed. Engl.* **1995**, *34*, 217.
(6) Mackay, L. G.; Wylie, R. S.; Sanders, J. K. M. *J. Am. Chem. Soc.* **1994**, *116*, 3141.
(7) Vidal-Ferran, A.; Clyde-Watson, Z.; Bampos, N.; Sanders, J. K. M. *J. Org. Chem.* **1997**, *62*, 240.
(8) Marvaud, V.; Vidal-Ferran, A.; Webb, S. J.; Sanders, J. K. M. *J. Chem. Soc., Dalton Trans.* **1996**, 985.

S0020-1669(97)01235-4 CCC: $14.00

Chart 1

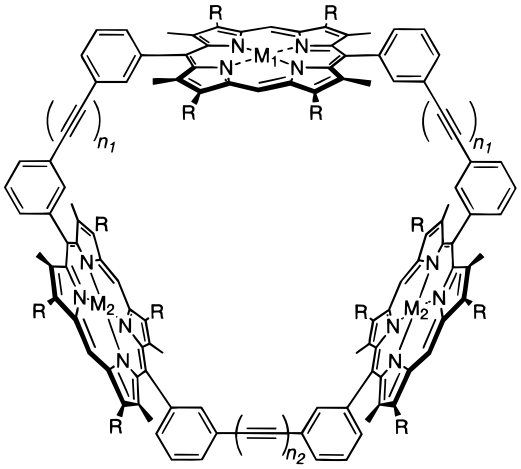

$Zn_3$1 (2,2,2-trimer, $n_1 = n_2 = 2$, $M_1 = M_2 = Zn$)
$Zn_3$2 (1,1,1-trimer, $n_1 = n_2 = 1$, $M_1 = M_2 = Zn$)
$H_6$3 (1,1,2-trimer, $n_1 = 1$, $n_2 = 2$, $M_1 = M_2 = H_2$)
$Zn_3$3 (1,1,2-trimer, $n_1 = 1$, $n_2 = 2$, $M_1 = M_2 = Zn$)
H_4Ni3 (1,1,2-trimer, $n_1 = 1$, $n_2 = 2$, $M_1 = Ni$, $M_2 = H_2$)
Ni$Zn_2$3 (1,1,2-trimer, $n_1 = 1$, $n_2 = 2$, $M_1 = Ni$, $M_2 = Zn$)
R = CH_2CH_2COOMe

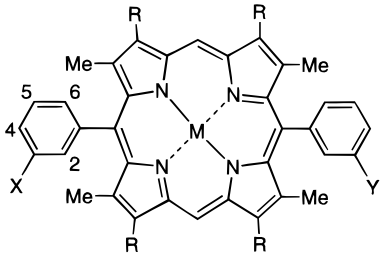

Zn4 (X = Y = C≡$CSiMe_3$, M = Zn)
Zn5 (X = I, Y = C≡$CSiMe_3$, M = Zn)
Zn6 (X = Y = I and M = Zn)
Zn7 (X = Y = C≡CH, M = Zn)
Ni7 (X = Y = C≡CH, M = Ni)
R = CH_2CH_2COOMe

as the central metal ion in this new family of host molecules, as it is easy to insert, gives stable monomer building blocks, and is expected to exhibit a much lower affinity for nitrogen-containing ligands than zinc (for piperidine, $K \approx 200$ M^{-1} in toluene at 22 °C).[9,10]

Results and Discussion

Synthesis. The synthesis of the Zn_3-1,1,2-trimer **$Zn_3$3** by the stepwise convergent route (Scheme 1) was initially investigated as model toward the synthesis of **Ni$Zn_2$8**.[11] A key fragment in the strategy was the unsymmetrical porphyrin monomer **Zn5**, which was synthesized using a mixed aldehyde route (Scheme 2). The dihydrodipyrrin **10** was prepared using literature procedures and converted to its α-free analogue **12** by palladium−carbon-catalyzed hydrogenolysis, followed by TFA-induced decarboxylation.[12] The α-free dipyrrole **12** was not isolated but condensed *in situ* with an equimolar mixture of the two aldehydes **11** and **13** using TFA as the catalyst, followed by DDQ oxidation.[13] A statistical mixture of **$H_2$4**, **$H_2$5**, and **$H_2$6** (1:2:1) was isolated in 64% yield. This procedure gave the porphyrin mixture on the gram scale, which was consequently metalated using zinc acetate in chloroform. The three monomers were separated chromatographically in the final step, as the metalated form of the porphyrins gave the best separation.

Deprotection of **Zn4** using TBAF gave **Zn7** (Chart 1) in high yield, which was then coupled to **Zn5** using $Pd(PPh_3)_4$, CuI, and NEt_3 to give linear trimer **$Zn_3$8** in 84% yield.[14] The efficient removal of the two TMS groups in linear trimer **$Zn_3$8** with TBAF (95% yield) and intramolecular Glaser−Hay coupling in CH_2Cl_2 using CuCl·TMEDA[13] in an atmosphere of dry air afforded the 1,1,2-cyclic trimer **$Zn_3$3** in 45% yield. Extended reaction times (14 h) were required in order to complete the cyclization of the unprotected linear trimer relative to those needed for the preparation of the Zn_3 2,2,2-trimer **$Zn_3$1**, perhaps reflecting greater strain in formation of the smaller cavity; this strain is predicted by CPK modeling. Addition of a template (*s*-tri(4-pyridyl)triazine, **Py_3T**, Chart 2) significantly improved the efficiency of the cyclization step (up to 65%). The template molecule, which fits efficiently into the cavity according to CPK models, kinetically drives *intra*molecular coupling by bringing together the two acetylene groups and, in doing so, minimizes *inter*molecular coupling. From UV binding studies (CH_2Cl_2 at 25 °C), the affinity for **Py_3T** by the linear (**$Zn_3$9**) and cyclic (**$Zn_3$3**) trimers (*ca.* 7×10^8 and 5×10^9 M^{-1}, respectively, see Table 1) provides a thermodynamic driving force for the templated cyclization. In the next step, demetalation was necessary in order to remove the template and facilitate chromatographic purification, after which the free-base 1,1,2-trimer **$H_6$3** (Chart 1) was remetalated to give the **$Zn_3$3** cyclic trimer in near quantitative yield.

The success of the synthesis described above allowed for the substitution of one Zn porphyrin by a Ni analogue, using **Ni7** (Chart 1) as the starting fragment. In doing so, the 1,1,2-linear trimer containing Ni in the central position, **Ni$Zn_2$8**, was obtained in 74% yield. TBAF deprotection was achieved in near quantitative yield, and the unprotected trimer was cyclized using CuCl·TMEDA−CH_2Cl_2 and **Py_3T** as the template. The zinc porphyrins were selectively demetalated by treatment with a dilute TFA solution to facilitate chromatographic purification. Under dilute acidic conditions, the Ni(II) porphyrin was

(9) LaMar, G. N.; Walker, F. A. In *The Porphyrins*; Dolphin, D., Ed.; Academic Press: New York, 1979; Vol. IV, pp 129−130.
(10) Walker, F. A.; Hui, E.; Walker, J. M. *J. Am. Chem. Soc.* **1975**, *97*, 2390.
(11) Vidal-Ferran, A.; Müller, C. M.; Sanders, J. K. M. *J. Chem. Soc., Chem. Commun.* **1994**, 2657; **1996**, 1849.
(12) (a) Young, R.; Chang, C. K. *J. Am. Chem. Soc.* **1985**, *107*, 898. (b) Abdalmunhdi, I.; Chang, C. K. *J. Org. Chem.* **1985**, *50*, 411. (c) Clezy, P. S.; Liepa, A. J. *Aust. J. Chem.* **1970**, *23*, 2443. (d) Czurylowski, M. Ph.D. Thesis, University of Freiburg, Switzerland, 1987.
(13) Anderson, H. L.; Sanders, J. K. M. *J. Chem. Soc., Perkin Trans. 1* **1995**, 2223.
(14) For examples of other large structures prepared using Pd-coupling, see: (a) Prathapan, S.; Johnson, T. E.; Lindsey, J. *J. Am. Chem. Soc.* **1993**, *115*, 7519. (b) Zhou, Z.; Kahr, M.; Walker, K. L.; Wilkins, C. L.; Moore, J. S. *J. Am. Chem. Soc.* **1994**, *116*, 4537.

Scheme 1

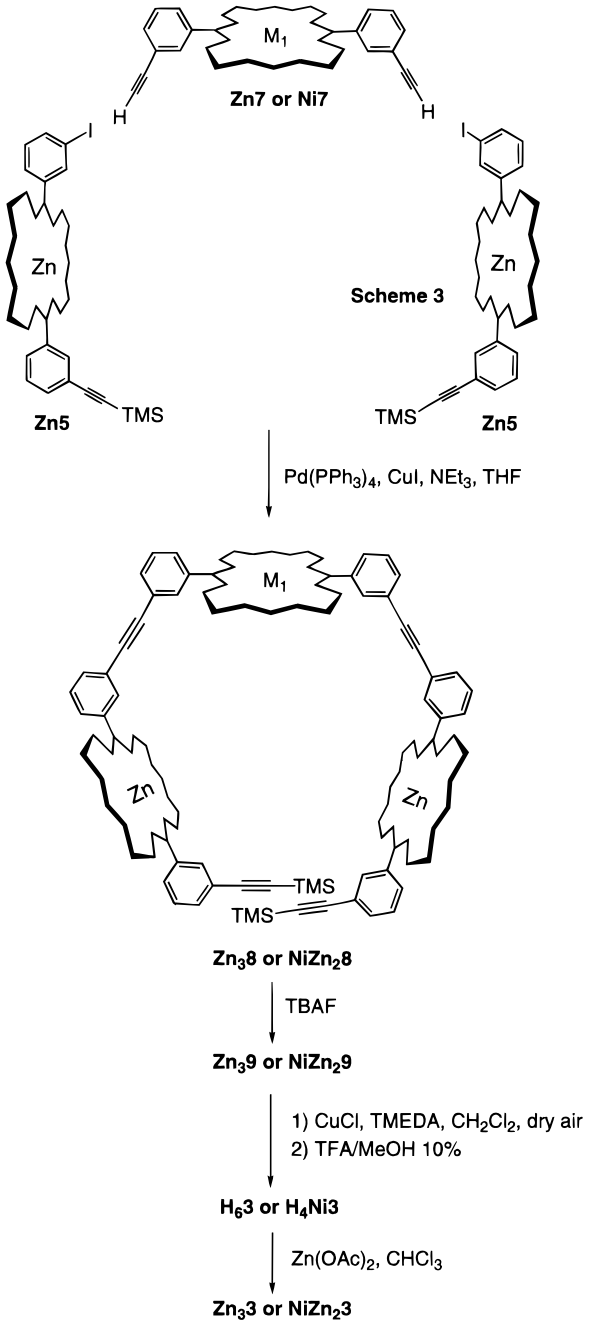

Scheme 2

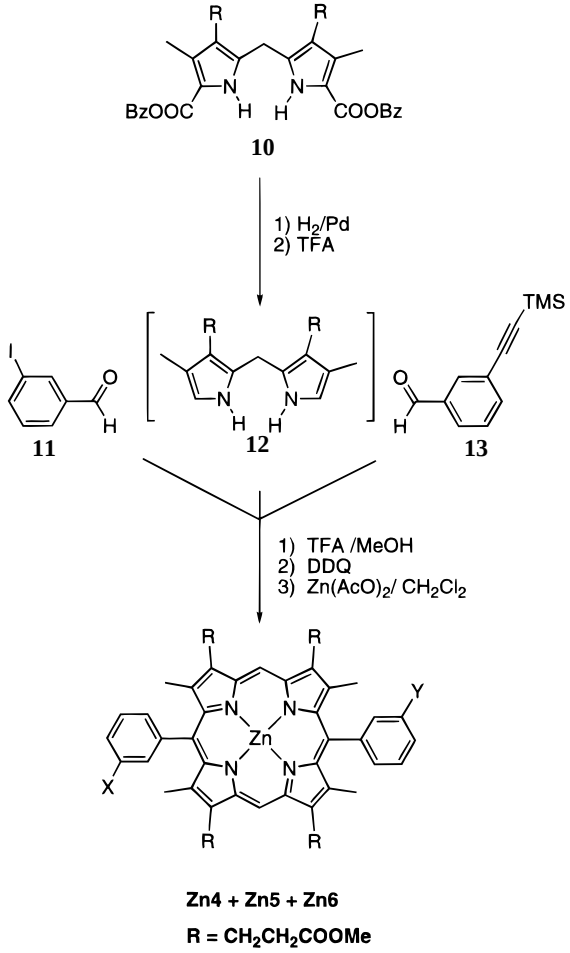

Chart 2

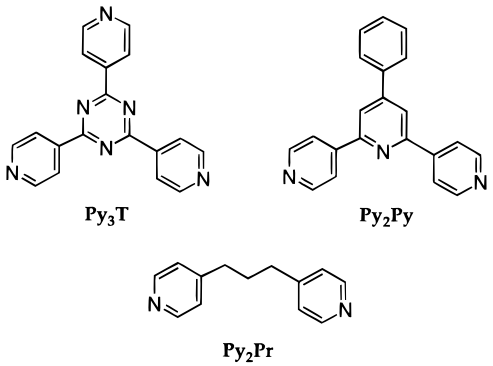

unaffected, and **H$_4$Ni3** (Chart 1) was obtained in 75% yield. Further treatment of the **H$_4$Ni3** trimer with Zn(II) acetate in chloroform yielded the final 1,1,2-cyclic trimer, **NiZn$_2$3** (Chart 1). The yield of the cyclization is higher in this case than for **H$_6$3**. The thermodynamic driving force for the templated cyclization would be greater for the $NiZn_2$ linear trimer relative to the Zn_3 linear trimer, as the difference in the binding constants for the linear and cyclic $NiZn_2$ 1,1,2-trimers with **Py$_3$T** is larger (*ca.* 6×10^6 M^{-1} for **NiZn$_2$9** and 5×10^9 M^{-1} for **NiZn$_2$3**, see Table 1). This might account for the higher efficiency in the ring-closure step.

Characterization of Zn$_3$3 and NiZn$_2$3. Unlike the symmetrical Zn_3 2,2,2-trimer, both the Zn_3 1,1,2-trimer and the $NiZn_2$-1,1,2-trimer possess two planes of symmetry (C_{2v} symmetry group), rendering two of the three porphyrins equivalent, an observation clearly manifest in the ^{1}H NMR spectrum. **Zn$_3$3** shows two partially resolved *meso* signals in a 1:2 ratio (at 9.98 and 10.00 ppm, respectively) and a complex aromatic region containing the 12 nonequivalent phenyl protons (the molecule contains three nonequivalent *ABCD* systems which will be abbreviated as I, II, and III in the discussion; see Figure 1). In the aliphatic region, the methylene groups of the ester side chains appear as two broad resonances, making the assignment of the three nonequivalent ester chains difficult. As expected, three resonances for the methyl groups of the porphyrin units were

Table 1. Empirical Ligand Affinities (M^{-1}) of Porphyrins in CH_2Cl_2 at 25 °C

	Py$_2$Py	Py$_2$Pr	Py$_3$T
Zn$_3$2 (1,1,1-cyclic trimer)	3×10^8	2×10^9	
Zn$_3$3 (1,1,2-cyclic trimer)	4×10^8	2×10^9	5×10^9
NiZn$_2$3 (1,1,2-cyclic trimer)	2×10^8	8×10^8	5×10^9
Zn$_3$1 (2,2,2-cyclic trimer)	5×10^8 (ref 25)	6×10^8 (ref 25)	
Zn$_3$9 (1,1,2-linear trimer)			7×10^8
NiZn$_2$9 (1,1,2-linear trimer)			6×10^6

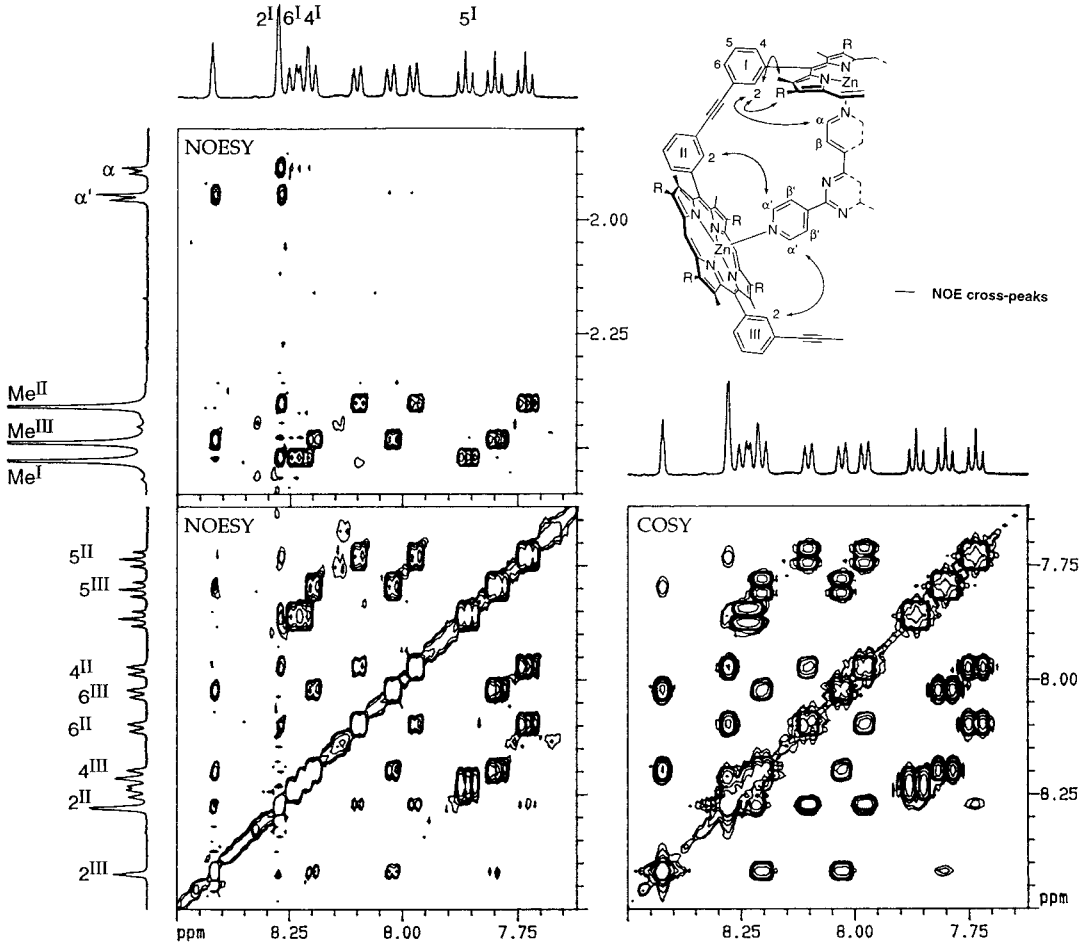

Figure 1. (Top right) Schematic representation of a fragment (through plane of symmetry) of the **$Zn_3$3**−**Py_3T** complex, showing significant connectivities (through space) from NOESY. (Bottom right) Aromatic region of the gradient COSY spectrum (500 MHz, $CDCl_3$, 300 K, magnitude mode), showing complete coupled systems for each of the phenyl groups. (left) Aromatic and aliphatic regions of the NOESY spectrum (500 MHz, $CDCl_3$, 300 K, $\tau_m = 1.2$s), showing significant through-space connectivities. Cross-peaks are identified between phenyl group and the porphyrin to which they are bound. Unfortunately, cross-peaks between phenyl resonances across an acetylene are not identified. As a result, the assignment of fragments II and III is arbitrary.

observed (at 2.36, 2.43, and 2.45 ppm), while the MeO groups of the ester chains were observed as three partially resolved singlets (at 3.54, 3.55, and 3.56 ppm). The ^{1}H NMR spectrum of the Ni-containing porphyrin in **$NiZn_2$3** also appears sharp. The *meso* resonances of the two equivalent Zn components were the same as in **Zn_3** (10.19 ppm), while the *meso* proton of the nickel porphyrin moves to lower chemical shift (9.38 ppm). The aromatic region remains congested, whereas in the aliphatic region the methylene signals of the ester side chains appear at unique chemical shifts (2.85 and 3.91 ppm for the methylene signals bonded to the nickel porphyrin and 3.08 and 4.31 ppm for the Zn components). The three nonequivalent methyl and methoxy groups of **$NiZn_2$3** were observed as well-separated signals (2.21, 2.47, and 2.56 ppm for the methyl groups and 3.56, 3.60, and 3.62 ppm for the methoxy protons; in these two sets of signals, the substituents in the Ni(II) component were shifted upfield).

Characterization of $Zn_3$3 and $NiZn_2$3 Py_3T Complexes. The addition of a stoichiometric quantity of **Py_3T** to a solution of **$Zn_3$3** led to dispersion of the resonances (particularly the aromatic region, in which three nonequivalent *ABCD* systems can be observed). Two *meso* signals (intensity ratio 2:1 at 9.82 and 9.87 ppm, respectively) and six equal intensity methyl peaks (three ester methyls at 3.44, 3.45, and 3.46 ppm and three ring methyl groups at 2.39, 2.48, and 2.50 ppm) were observed, as expected from the predicted symmetry (Figure 1). The strength of binding to this class of cyclic trimers is demonstrated by the presence of two sharp sets of multiplets for the bound ligand, with intensity ratio 2:1, as the intramolecular exchange of the pyridyl groups by rotation within the cavity is occurring remarkably slowly. The upfield shifts for Hβ are observed at 7.00 ($\Delta\delta$ −1.55) and 7.05 ($\Delta\delta$ −1.50) ppm and for Hα at 2.73 ($\Delta\delta$ −6.20) and 2.76 ($\Delta\delta$ −6.17) ppm (Figure 1). These shifts are slightly greater than those for the 2,2,2-trimer **$Zn_3$1**, as might be expected for the closer average proximity of the ligand to the porphyrin units of the smaller cavity. Complete characterization of all the resonances was achieved with the aid of 2D-NMR spectroscopy (COSY and NOESY, see Figure 1), where COSY made assignment of the three *ABCD* aromatic systems relatively simple. The Hα signal of **Py_3T** exhibited NOE cross-peaks to H2 in ring I (from NOESY, see Figure 1), which in turn allowed the assignment of the resonances of porphyrin I (methyl, methylene, and aromatic *ABCD* system), while the Hα' resonances gave NOE cross-peaks to the two remaining H2 protons (in ring II and ring III, which in turn identify their respective neighboring methyl and methylene resonances). The lack of cross-peaks between the resonances attributed to ring I and the resonances of either ring II or III did not allowed us to assign with certainty the aromatic system neighboring ring I. However, the absence of NOE cross-peaks between the H2 signal at 8.42 ppm and the overlapping H2 signals at 8.28 ppm belonging to ring I and ring II or III, respectively, suggests that the less intense H2 signal belongs to ring III.

The stoichiometric addition of **Py_3T** to a chloroform solution of **$NiZn_2$3** gave a ^{1}H NMR spectrum quite different in appearance from that for the **Zn_3** analogue. The peaks attributed to the nickel porphyrin became relatively broad,[15] with the chemical shifts for some of these resonances deviating significantly from their positions in the free host. Most dramatically shifted was the *meso* resonance of the nickel porphyrin, which at room temperature appeared at 14.5 ppm ($W_{1/2} \approx 25$ Hz). The remaining resonances assigned to the zinc porphyrin components of the cyclic host remain largely unaffected, allowing assignment of the peaks, though the absolute assignment of the II and III components is not trivial (due to the symmetry properties of the molecule, described earlier). A similar analysis of the ^{1}H-NMR spectrum of the 1:1 complex of $NiZn_2$ 1,1,2-cyclic trimer with **Py_2Py** (Chart 2) also failed to give diagnostic NOESY cross-peaks, although the relative assignment of the porphyrin fragments is beyond dispute. This observation implies complexation of the pyridyl component of the **Py_3T** ligand. In order to explain this observation, we need to consider the properties of a nickel porphyrin monomer.

In the absence of nitrogenous ligands, nickel(II) porphyrin monomers, like the zinc analogues, are stable, four-coordinate, square-planar complexes; there is inconclusive evidence for the formation of a five-coordinate species.[10,16−19] The addition of a suitable ligand (such as pyridine) establishes an equilibrium between the four-coordinate diamagnetic nickel complex and a paramagnetic hexacoordinate product, where the progress of the reaction can be followed spectroscopically.[18,20] The position of the equilibrium varies as a function of ligand basicity, porphyrin structure, and temperature. For example, the complex stability is inversely related to the ligand base strength,[16,18] or, to put it another way, the strength of ligand binding increases as a function of the decrease in the pyrrolic nitrogen basicity of the free-base porphyrin.[18] Interpretation of ligand binding, though, is sometimes counterintuitive. For example, piperidine is 10^6 times more basic than pyridine, yet the stability constants of porphyrin−piperidine complexes are only about twice as large as those of the pyridine analogues.[16] This has been attributed to the nature of the bond formed, whereby the pyridine lone pair donation results in a charged species. In addition to the ligand, the substituents on the porphyrin periphery play a crucial role in the complex stability. Electron-withdrawing groups increase the strength of chelation of the metal to the porphyrin and the ligand to the metal, forcing the equilibrium in favor of the dipyridyl complex, contrary to what would be expected if the metal−nitrogen bond was ionic.[16,18,20]

The equilibrium will also be driven by the relative solvation energies of the species in solution. In polar solvents, for most tetrasubstituted synthetic porphyrins, the four-coordinate species will be preferred to the dipyridinate complex, which will present the back of two pyridine molecules and the nonpolar periphery of the porphyrin.[16] This effect will naturally vary as the polarity of porphyrin substituents changes.

In the square-planar configuration, all eight nickel d electrons are spin-paired in the d_{xz}, d_{yz}, d_{x^2}, and d_{xy} orbitals, leaving the high-energy $d_{x^2-y^2}$ orbital unoccupied and resulting in an overall diamagnetic complex. The porphyrin can be considered a strong-field ligand, as the square-planar complex is the preferred form. The d_{xz} and d_{yz} orbitals (each of *e* symmetry by virtue of the 4-fold symmetry) are fully occupied and are of the correct symmetry to overlap with the porphyrin π orbitals. This allows for d_π back-donation interactions with the π^* orbitals of the porphyrin (M → L π back-donation). Such charge transfer drives spin density into the porphyrin orbital of $4e(\pi^*)$ symmetry and, as a result, places the greatest spin density at the *meso* position, giving characteristic large shifts of the *meso* proton.[21] From this interaction, it is feasible to see that electron density can transmit from the metal to the porphyrin periphery (and *vice versa*). But, in the square-planar configuration, the d_{xz}, d_{yz}, and d_{z^2} orbitals are of comparable energy, retarding the complexation of any further ligands. In the octahedral configuration, however, the d_{z^2} orbital is higher in energy than the d_{xz}, d_{yz}, and d_{xy} orbitals and degenerates with the $d_{x^2-y^2}$ orbital (e_g) both singly occupied and resulting in an overall paramagnetic system. Approach of two ligands (which will lead to a hexacoordinate complex) will build up electron density at the metal center. It is the delocalization of this electron density onto the porphyrin ring (through $d_\pi-\pi^*$ back-donation) that drives the formation of the octahedral complex; i.e., the net effect is to lower the energy of the d_{z^2} orbital, which ultimately drives the formation of the octahedral complex. A further consequence is the spin delocalization of the metal-centered paramagnetism to sites on the periphery of the porphyrin ring.

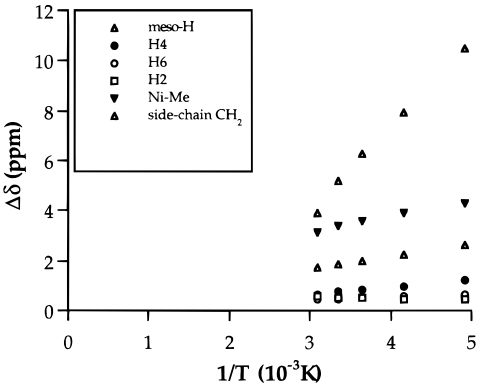

Figure 2. Plot of the isotropic shifts as a function of (inverse) temperature (Curie plot) for resonances of the nickel porphyrin component of the **$NiZn_2$3**−**Py_3T** complex (400 MHz, $CDCl_3$). Assignment of the resonances is presented in the monomer structure shown earlier in this text. The positions of the zinc porphyrin resonances are invariant to changes in temperature.

The ^{1}H-NMR spectrum of **$NiZn_2$3** gives broad resonances for the protons of the nickel porphyrin at room temperature which sharpen at lower temperatures, while resonances due to the two Zn-bearing porphyrins remain sharp throughout. The delocalization ($d_\pi-\pi^*$) described earlier populates specific sites on the porphyrin and contact shifts[11] at these sites describe the paramagnetic phenomenon in the octahedral Ni(II). The change in the isotropic shift as a function of T^{-1} (Figure 2) is linear for all proton resonances but deviates from ideal Curie behavior (lines do not intersect the origin), perhaps due to a dipolar shift contribution.[22] It has been suggested previously that the deviation is a property of a host rather than any temperature-dependent equilibrium between the mono- to bis-ligand complex.[22] The formation of the five-coordinate porphyrin complex would require the nickel to sit out of the plane of the porphyrin[23]

(15) Milgrom, L. R.; Dempsey, P. J. F.; Yahioglu, G. *Tetrahedron* **1996**, *52*, 9877.
(16) Storm, C. B.; Corwin, A. H.; Arellano, R. R.; Martz, M.; Weintraub, R. *J. Am. Chem. Soc*. **1966**, *88*, 2525.
(17) Kirksey, C. H.; Hambright, P.; Storm, C. B. *Inorg. Chem.* **1969**, *8*, 2141.
(18) Caughey, W. S.; Fujimoto, W. Y.; Johnson, B. P. *Biochemistry* **1966**, *5*, 3830.
(19) Miller, J. R.; Dorough, G. D. *J. Am. Chem. Soc.* **1952**, *74*, 3977.
(20) McLees, B. D.; Caughey, W. S. *Biochemistry* **1968**, *7*, 642.
(21) (a) Shulman, R. G.; Glarum, S. H.; Karplus, M. *J. Mol. Biol.* **1971**, *57*, 93. (b) Bell, S. E.; Aakeröy, C. B.; Al-Obaidi, A. H. R.; Hegarty, J. N. M.; McGarvey, J. J.; Lefley, C. R.; Moore, J. N.; Hester, R. *J. Chem. Soc., Faraday Trans*. **1995**, *91*, 411.
(22) La Mar, G. N.; Walker, F. A. *J. Am. Chem. Soc.* **1973**, *95*, 1782.

Scheme 3

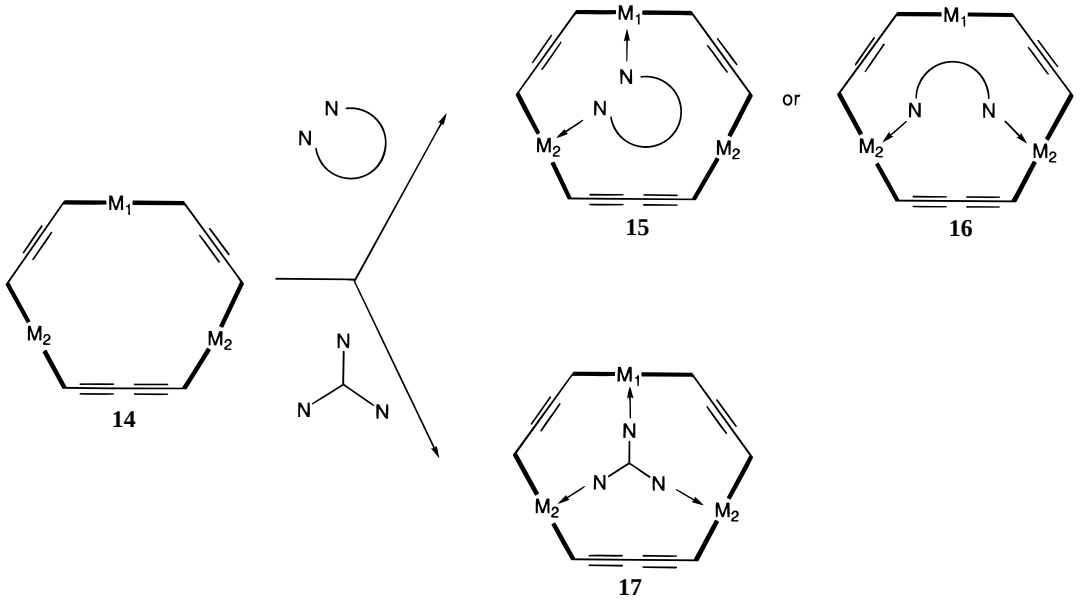

and, as a result, destabilize the $d_\pi-\pi^*$ overlap. Such species, though postulated from UV studies, have been generated by electroreduction of Ni(II) porphyrins.

The influence of the substituents on the porphyrin periphery (described above) will now play a critical role on the stability of the octahedral product. Electron-withdrawing groups will favor the formation of the octahedral complexes, as they will act to deplete the porphyrin of electrons and, thus, facilitate the delocalization of electron density from the electron-rich metal onto the porphyrin ring, as a result stabilizing the ligand−metal bond. In the systems investigated in this work, the acetylene-substituted aryl groups act as electron-withdrawing groups, which would, in effect, force the equilibrium to the right (though perhaps not as dramatically would as a nitro or oxo group).[24] This would lead us to expect little binding of a nitrogenous ligand to the nickel porphyrin, requiring a vast excess of ligand. The fact that the nickel porphyrin exhibits paramagnetism in the host molecule by addition of a stoichiometric amount **Py$_3$T** implies that the binding of two pyridyl groups of the ligands to the two Zn sites increases the effective molarity of the third pyridyl group at the Ni site, as a result forming a nickel−nitrogen bond. The lack of excess ligand implies the formation of a five-coordinate complex, but literature precedent suggests that the sixth site will be occupied by a solvent molecule ($CHCl_3$[10] or methanol,[18] both of which are present at various points in the sample preparation).

Binding Properties of Zn$_3$3 and NiZn$_2$3. A tridentate ligand with a complementary size and shape will tend to exhibit a three-site interaction with the host molecule (**17** in Scheme 3). An interesting question arises when considering the complexation of **NiZn$_2$3** and a tridentate ligand such as **Py$_3$T** as to whether binding will take place via a two- or three-site interaction. The nickel(II) center exhibits a low affinity for pyridine-containing ligands, and any binding interaction with such ligands only takes place at high ligand concentrations,[10] *ca.* 2−3 M pyridine in $CDCl_3$ from our NMR studies. However, the effective molarity of the third binding end of a tridentate ligand may well be high enough to form a "three-site complex", in effect from a stoichiometric quantity of ligand.

The binding properties of **Zn$_3$3** and **NiZn$_2$3** to several pyridine-containing bidentate and tridentate ligands were investigated, as a comparative study of the ligand affinity of a host molecule to a range of polydentate ligands provides valuable information concerning the shape and the size of the cavity of the host molecule. We have previously used a similar approach to study other porphyrin oligomers.[25,26] In general, the higher the ligand affinity, the greater the capacity for the cavity to accommodate the polydentate ligand, driven by the entropically favorable formation of many metal−ligand bonds. A representation of the complexation of a bidentate and a tridentate ligand to the cavity of 1,1,2-cyclic trimers **Zn$_3$3** (**14**, $M_1 = M_2 =$ Zn) and **NiZn$_2$3** (**14**, $M_1 =$ Ni, $M_2 =$ Zn) is shown in Scheme 3. A bidentate ligand can bind to **Zn$_3$3** in one of two ways given the C_{2v} symmetry of the molecule, where the chelation will occur between two porphyrins linked either by one ethyne, **15**, or one butadiyne unit, **16**. In such a scenario, the binding process in which the two porphyrin components of the trimer better accommodate the ligand will take place. The binding of **NiZn$_2$3** with a bidentate ligand will probably involve only the two porphyrins containing Zn (structure **16** in Scheme 3), given the "preference" of nitrogen-containing ligands for Zn(II) over Ni(II) porphyrins.[9b]

The binding of oligopyridyl ligands (*s*-tri(4-pyridyl)triazine, **Py$_3$T**, 4′-phenyl-4,2′:6′,4″-terpyridyl, **Py$_2$Py**; and 1,3-di(4-pyridyl)propane, **Py$_2$Pr**, Chart 2) to several porphyrin oligomers has been investigated using electronic and NMR spectroscopy. In order to aid discussion, the ligand affinities of the previously reported 2,2,2-cyclic trimer, **Zn$_3$1**,[25] and the 1,1,1-cyclic trimer, **Zn$_3$2**,[7] to the same pyridine-containing ligands have been included (cyclic trimers **Zn$_3$3** and **NiZn$_2$3** will be smaller than **Zn$_3$1** by two ethyne units but larger than **Zn$_3$2** by one ethyne unit). Ligand affinities were determined from UV titration curves.[25,27] Table 1 summarizes the empirical ligand affinities (M^{-1}) in dichloromethane at 25 °C. High binding constants become difficult to measure by UV/vis spectroscopy, and virtually all the values determined in this study were in the

(23) Kadish, K. M.; Franzen, M. M.; Han, B. C.; Araullo-McAdams, C.; Sazou, D. *Inorg. Chem.* **1992**, *31*, 4399.
(24) McCallien, D. W. J.; Sanders, J. K. M. *J. Am. Chem. Soc.* **1995**, *117*, 6611.
(25) Anderson, H. L.; Sanders, J. K. M. *J. Chem. Soc., Perkin Trans. 1* **1995**, 2231.
(26) (a) Anderson, H. L.; Hunter, C. A.; Meah, M. N.; Sanders, J. K. M. *J. Am. Chem. Soc.* **1990**, *112*, 5780. (b) Anderson, H. L. *Inorg. Chem.* **1994**, *33*, 972.
(27) Connors, K. A. *Binding Constants*; Wiley: Chichester, 1987; p 51.

region $>1 \times 10^8$ M^{-1}. Care was taken to minimize random and systematic errors, as extremely dilute solutions were needed for measuring the binding affinities (see Experimental Section). Each binding constant was measured at least twice, and the values were found to be reproducible to within ±50%, the main factors limiting reproducibility being inaccurate volume addition, ligand concentration error, and solvent evaporation during the course of titration.

The binding constants for **Py_2Pr** and all the host molecules studied were found to be relatively high ($>1 \times 10^8$ M^{-1}). The combined UV data set from the titration was analysed for simple 1:1 association. **Zn_31** (2,2,2-cyclic trimer) and **$NiZn_23$** (1,1,2-cyclic trimer) were found to have almost identical binding constants, where the binding of **Py_2Pr** to **$NiZn_23$** must be taking place principally between the two zinc porphyrins (structure **16** in Scheme 3), given the preference of pyridine to bind to Zn(II) over Ni(II). The dominant contribution in both the **Zn_31** and **$NiZn_23$** binding processes must be the **Py_2Pr** ligand spanning the two porphyrin units separated by a butadiyne unit, which would explain the similar ligand affinities for the **Zn_31**− and **$NiZn_23$**−**Py_2Pr** complexes. The remaining two host molecules investigated, **Zn_31** (1,1,1-cyclic trimer) and **Zn_33** (1,1,2-cyclic trimer) were found to have identical **Py_2Pr** ligand affinities (2×10^9 M^{-1}), though they were higher than those for **Zn_31** and **$NiZn_23$** (see Table 1). The comparable binding geometry in both cases suggests that the binding is taking place between the two porphyrins separated by one ethyne group. **Zn_33** has two options for accommodating bidentate ligands: in the first, the ligand spans a monoacetylene subfragment (structure **15**, Scheme 3) while in the second, the ligand spans the bisacetylene subfragment (structure **16**, Scheme 3). It then follows that the ligand will bind with a 1,1,1- or 2,2,2-trimer-like geometry, depending on which of the two configurations accommodates it best.

The data presented in Table 1 suggest that **Py_2Py** shows little preference for any one particular host, as the binding affinities across the series are quite similar (within experimental error) ($\sim 10^8$ M^{-1}, see Table 1).

The **Py_3T** ligand is particularly interesting because of its size and shape complementarity with the cavity of the trimeric hosts; this ligand is, in fact, used as a template in the formation of the cavities investigated in this work. As expected, **Py_3T** was found to bind very efficiently to all the trimeric hosts, **Zn_33**, **$NiZn_23$**, and **Zn_32** (1,1,1-cyclic trimer), with binding affinities higher than 1×10^9 M^{-1}.[28] In this regime, it becomes very difficult to measure binding constants by UV/vis spectroscopy; however, a trend can be established in the empirical ligand affinities, with the binding affinity increasing upon progressive reduction in the size of the cavity; this proposition agrees with molecular modeling.

NMR Competition Experiments. In order to establish the relative binding affinities of **Py_3T** to the three trimeric hosts **Zn_31**, **Zn_32**, and **Zn_33**, two competitive NMR binding experiments were undertaken. In the first, addition of 1 equiv of Zn_3 1,1,2-trimer to a solution of the 1:1 Zn_3 2,2,2-trimer−**Py_3T** complex (~2 mmol, $CDCl_3$) resulted in complete transfer of the **Py_3T** ligand to the smaller cavity, almost instantaneously

Scheme 4

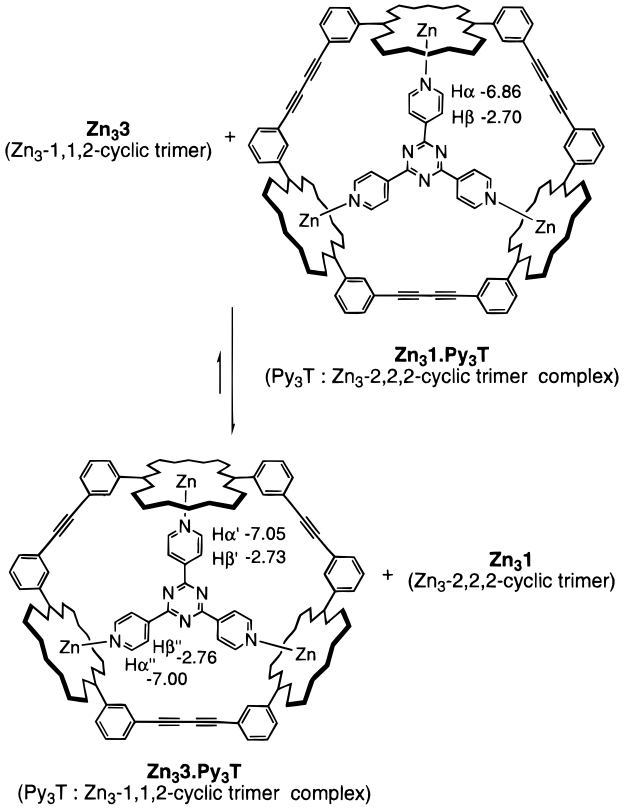

(Scheme 4). Addition of 1 equiv of Zn_3 2,2,2-trimer to a solution of the 1:1 **Py_3T**−**Zn_33** complex resulted, as expected, in no net transfer of the ligand. This proves that the binding affinity of **Py_3T** for **Zn_33** is higher than that for **Zn_31**. An accurate value for the ratio of the binding constants cannot be derived from these experiments, though it is safe to predict that the binding constant of **Py_3T** to the smaller Zn_3 1,1,2-trimer is at least an order of magnitude greater than that to the larger Zn_3 2,2,2-trimer.

In the second competition experiment (Scheme 5), addition of 1 equiv of the Zn_3 1,1,1-trimer to a solution containing 1 equiv of the 1:1 Zn_3 1,1,2-trimer−**Py_3T** complex and 1 equiv of Zn_3 2,2,2-trimer does not result in the expected rapid transfer of the **Py_3T** ligand to the smaller 1,1,1 cavity. In fact, the ligand transfer did not take place at room temperature, as the dissociation rate of the starting 1:1 complex must be low. After heating of the solution for 120 h at 60 °C, only 23% of the **Zn_33** (1,1,2-trimer)-bound **Py_3T** was "transferred" into the smaller **Zn_31** cavity. The ring-current-induced shifts for **Py_3T** in all the ligand−trimer complexes are shown in Scheme 5. In this case, it can also be predicted that the binding constant of **Py_3T** to the smaller Zn_3 1,1,1-trimer is larger than that to Zn_3 1,1,2-trimer. NMR binding studies confirm the relative trend observed by electronic spectroscopy studies, which is that the smaller the cavity, the higher the ligand affinity.

Conclusions

The coupling of asymmetric porphyrin monomers to give trimers provides a general route for the preparation of mixed metal hosts.[29] For **$NiZn_23$**, while the ^1H NMR ligand−metal resonances of the free host appear sharp, addition of the tridentate guest **Py_3T** resulted in significant broadening of the resonances due to the nickel-containing fragment. This unexpected result leads us to conclude that the cavity-enforced effective molarity of the third pyridyl of **Py_3T** at the Ni binding

(28) A higher binding constant for **Py_3T** and **Zn_31** (2,2,2-cyclic trimer) has been already published in the range 4×10^9−5×10^{10} M^{-1} according to UV and NMR measurements (ref 24). This value is higher than the one measured in this work for the same binding process (see Table 1). This inconsistency in the empirical value from different experimentalists ultimately reflects the fact that such high empirical affinities must be regarded only as order of magnitude estimates (reproducible within experimental error). With such high binding constants, comparisons can only be made on a relative scale.

Scheme 5

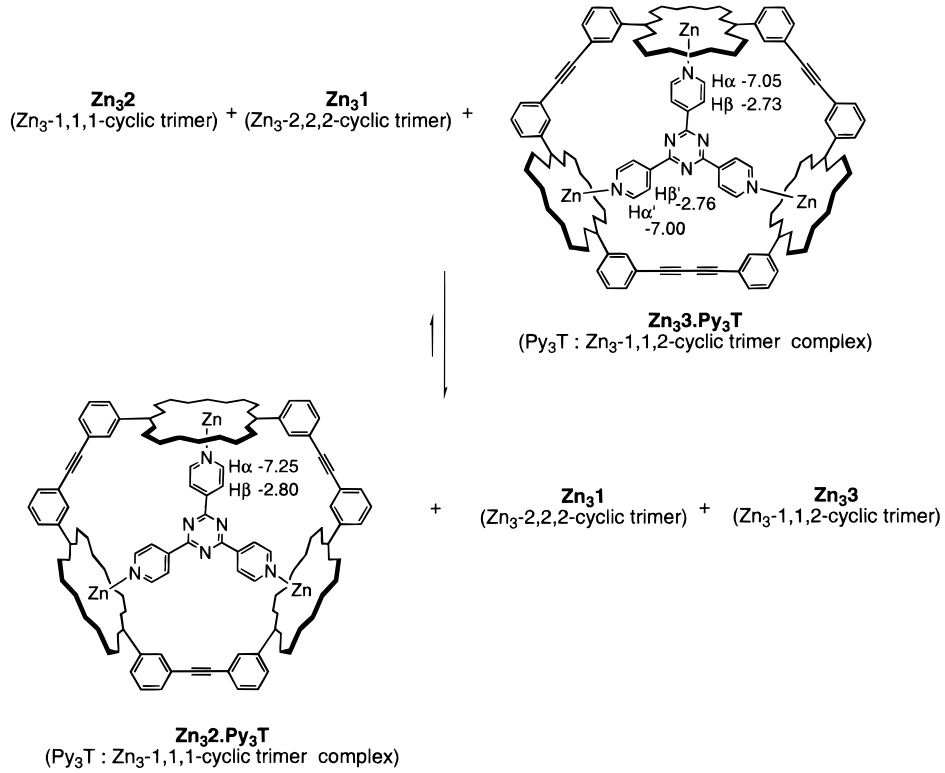

site is high enough to form a nickel−pyridyl bond. The resulting Ni(II) complex has paramagnetic properties and has been characterized by NMR.

Experimental Section

^{1}H NMR spectra were recorded on Bruker WM-250, AM-400, or DRX-500 spectrometers in deuteriochloroform operating at 250, 400, or 500 MHz respectively, while ^{13}C NMR spectra were obtained on an AM-400 operating at 100 MHz. Deuteriochloroform was deacidified before use by storage over anhydrous potassium carbonate. Chemical shifts are quoted relative to residual solvent (7.25 ppm for ^{1}H and 77.0 ppm for ^{13}C of $CDCl_3$), and coupling constants (*J*) are given in hertz. IR spectra were recorded on a Perkin-Elmer 1710 instrument in Fourier transform mode. UV/visible spectra were obtained on a Perkin Elmer Lambda 2 UV/vis spectrometer in 10 mm oven-dried cuvettes. Fast atom bombardment mass spectra (FAB MS) were obtained from the EPSRC service at Swansea.

Distilled solvents were used throughout and, when used dry, were freshly obtained from the solvent stills (CH_2Cl_2, MeOH, and NEt_3 from CaH_2, THF from $LiAlH_4$). All flash chromatography was carried out using 60 mesh silica gel and columns dry-packed. Thin-layer chromatography (TLC) was carried out on Kieselgel 60 PF_{254} (Merck) 0.2 mm plates. CuCl,[30] 3-trimethylsilylethynylbenzaldehyde,[31] 3-iodobenzaldehyde,[32] 5,5′-dibenzyloxycarbonyl-3,3′-di(2-methoxycarbonylethyl)-4,4′-dimethyl-2,2′-dipyrrylmethane,[12c] 4′-phenyl-4,2′:6′,4″-terpyridyl (**Py_2Py**)[33] and *s*-tri(4-pyridyl)triazine (**Py_3T**)[34] were prepared according to known procedures. The final purification step in all porphyrin preparations was crystallization by layered addition of methanol to a chloroform solution of the compound, followed by drying *in vacuo*.

General Procedure for the Preparation of Zinc Complexes. Free-base porphyrins were converted into the corresponding zinc complexes in near quantitative yield by treatment with excess zinc acetate dihydrate (5 equiv) in refluxing $CHCl_3$ (10 min). The mixture was allowed to cool and excess zinc acetate was removed by filtration. The porphyrins were then recrystallized by layered addition of methanol to a chloroform solution of the compound, filtered, and dried *in vacuo.*

General Procedure for the Cleavage of the TMS Protecting Groups. In this procedure, 1.1 equiv of tetrabutylammonium fluoride (as a 1 M solution in THF) was added in syringe into a CH_2Cl_2 solution of the porphyrin. The mixture was stirred at room temperature until no starting material was detected by TLC (*ca.* 1 h). Two spatulas of $CaCl_2$ were then added, and the mixture was stirred for 2 min and then washed with H_2O (2 × 25 mL). The organic solution was concentrated and layered with MeOH, and the porphyrin compound was filtered and dried (*in vacuo*).

General Procedure for the Measurement of Binding Constants by UV/Visible Titration. A solution of ligand in CH_2Cl_2 (*ca.* 10^{-6}−10^{-7} M) was added in portions *via* microsyringe to a CH_2Cl_2 solution of porphyrin host (*ca.* 10^{-7}−10^{-8} M, initial absorbance *ca.* 0.05−0.15) in a thermostated cuvette (25 °C). Absorbance readings were taken at two wavelengths, close to which maximum change occurred during the course of the titration: one wavelength at which the absorption declined near the λ_{max} of the free host (409 nm) and another wavelength at which the absorption rose near the λ_{max} of the complex (423 nm). One data set was subtracted from the other and the combined data set was used to carry out the simulation analysis. The use of the combined data set helps eliminate random errors accumulated throughout the course of the titration.[25] The Soret band of the porphyrin was red-shifted by *ca.* 15 nm on binding an oligopyridyl ligand. In contrast, the Ni(II) porphyrin Soret band did not shift noticeably on binding a nitrogen-containing ligand.[10] From 20 to 30 ligand additions were made adding *ca.* 2 equiv of the ligand overall. Ligand was added *via* syringe into the host solution in sufficiently small quantities so as to give readings evenly distributed along the curve. Ligand affinities were determined using a least-squares curve-fitting program.[35] The equation used for analyzing UV titration data corresponding to a 1:1 binding model, and taking into account changes in volume due to ligand

(29) Other metals (Ru, Pd, Sn) and modified building blocks (dioxo- and nitroporphyrins) have been successfully incorporated into trimers using this route: Webb, S. J.; ClydeWatson, Z.; Hawley, J. C.; Darling, S. L. To be published.
(30) Keller, R. N.; Wycoff, H. D. In *Inorganic Syntheses, Vol. II*; Fernelius, W. C., Ed.; McGraw-Hill Book Co., Inc.: New York, 1946; p 1.
(31) Austin, W. B.; Bilow, N.; Kellegham, W. J.; Lau, K. S. Y. *J. Org. Chem.* **1981**, *46*, 2280.
(32) Barker, I. R. L.; Waters, W. A. *J. Chem. Soc.* **1952**, 150.
(33) (a) Kröhnke, F. *Synthesis* **1976**, 1. (b) Awartani, R.; Sakizadeh, K.; Gabrielsen, B. *J. Chem. Educ.* **1986**, *63*, 172.
(34) (a) Biedermann, H.; Wichmann, K. *Z. Naturforsch., B* **1986**, *29*, 360. (b) Anderson, H. L.; Anderson, S.; Sanders, J. K. M. *J. Chem. Soc., Perkin Trans. 1* **1995**, 2231.

addition, was of the general form

$$A_{exp} = \frac{A_0 + A_f K L_{free}}{1 + K L_{free}}$$

where A_{exp} is the experimental absorbance, A_0 is the initial absorbance, A_f is the final fully bound absorbance, K is the binding constant, and L_{free} is the free ligand concentration, which is calculated by solving the following quadratic equation:

$$K L_{free}^2 + L_{free}(1 + K(M_0 - L_0)) - L_0 = 0$$

where M_o is the starting porphyrin concentration and L_o is the starting ligand concentration.

Each binding constant was measured at least twice. The values were reproducible to within ±50%, the main factors limiting reproducibility being inaccurate volume addition, ligand concentration, and evaporation loss during the course of titration.

Preparation of Zn4, Zn5, and Zn6. Palladium on carbon (750 mg, 10%) was added to a solution of 5,5′-bis[(benzyloxy)carbonyl]-3,3′-bis[(2-methoxycarbonyl)ethyl]-4,4′-dimethyl-2,2′-dipyrrylmethane[12c] (12.30 g, 0.02 mol) in THF (125 mL, distilled from $LiAlH_4$) containing 1% triethylamine. The mixture was stirred under hydrogen for 3 h. The catalyst was filtered and the filtrate evaporated before drying under vacuum for 3 h. The residue was cooled to 0 °C (ice bath), and 100 mL of degassed TFA (three freeze−thaw cycles) was added *via* canula under argon. The mixture was stirred vigorously at 0 °C for 20 min and allowed to stir at 20 °C for a further 20 min. Periodically, the reaction vessel was evacuated and Ar introduced in order to remove CO_2. At this stage, the dark orange solution was cooled to −25 °C (ice, dry-ice, acetone). A degassed solution of an equimolar mixture of 3-iodobenzaldehyde (2.32 g, 0.01 mol) and 3-[(trimethylsilyl)ethynylbenzaldehyde (2.02 g, 0.01 mol) in methanol (100 mL) was added to the cold solution of the dipyrromethane *via* canula. The mixture was left to stir for 2 h at −20 °C. The cold bath was removed and 2,3-dichloro-5,6-dicyano-1,4-benzoquinone (4.70 g, 20.6 mmol) added, followed with $CHCl_3$ (50 mL), and the mixture was stirred for 10 min. CH_2Cl_2 (1 L) and Et_3N (100 mL) were then added with great care (*CAUTION*: exothermic reaction). The organic solution was washed with H_2O (2 × 500 mL), the solvent removed, the residue dried *in vacuo* for 0.5 h, and the solution finally chromatographed through SiO_2, eluting with $CHCl_3$/NEt_3 (100:1). The main red band was collected, concentrated (to 40 mL), and crystallized to yield the porphyrin mixture (7.10 g, 65%; the yield of the reaction has been inconsistent, varying from 39 to 65%): ^{1}H NMR (250 MHz, $CDCl_3$) δ −2.50 (br s, exch. with D_2O, NH), 0.24 (s, Me_3Si), 2.52 and 2.54 (s, Me), 3.16 (t, J = 8.0 Hz, CH_2-CH_2-COOMe), 3.66 (s, MeO), 4.36 (t, J = 8.0 Hz, CH_2-CH_2-COOMe), 7.46−8.44 (m, 8H, aryl-*H*), 10.28 and 10.29 (s, meso-*H*). The free-base porphyrin mixture (1.69 g) was metalated, and the zinc porphyrins **Zn4**, **Zn5**, and **Zn6** were separated by chromatography through SiO_2, eluting with AcOEt/$CHCl_3$/hexane (1:1:2). **Zn4** was initially collected, followed by **Zn5**, and finally **Zn6**, all of which were recrystallized by layered addition of MeOH to a concentrated solution of the respective monomers. **Zn4** (315 mg, 72% for the metalation and separation steps), **Zn5** (535 mg, 69%, for the metalation, separation, and recrystallization steps), and **Zn5** (440 mg, 96% for the metalation and purification steps) were obtained.

The spectroscopic properties of **Zn4** were in agreement with the data previously reported.[2b]

Zn5: ^{1}H NMR (250 MHz, $CDCl_3$) δ 0.25 (s, 9H, $SiMe_3$), 2.49 and 2.50 (s, 12H, Me), 3.15 (t, J = 7.0 Hz, 8H, CH_2-CH_2-COOMe), 3.68 (s, 12H, MeO), 4.33 (t, J = 7.0 Hz, 8H, CH_2-CH_2-COOMe), 7.46−8.47 (m, 8H, aryl-*H*), 10.21 (s, 2H, meso-*H*); ^{13}C NMR (100 MHz, $CDCl_3$) δ 0.0 ($SiMe_3$), 15.7 (Me), 21.9 (CH_2-CH_2-COOMe), 37.0 (CH_2-CH_2-COOMe), 51.7 (MeO), 94.9 (C≡C-$SiMe_3$), 97.6 (*meso*-H), 105.1 (C≡C-$SiMe_3$), 118.0 and 119.0 (*meso*-aryl), 93.7 and 122.8 (aryl-I and aryl-C≡C), 127.7, 129.2, 132.0, 132.4, 133.1, 136.4, 137.5 and 142.0 (aryl-H), 138.9, 139.2, 141.6, 141.7, 146.05, 146.1, 147.4 and 147.7 (pyrrole), 143.3 and 145.6 (aryl-porph), 173.5 (*C*OOMe); FAB calcd for $C_{57}H_{60}O_8N_4ISiZn$ 1148.5 [M^+], found 1146; λ_{max} (CH_2Cl_2)/nm 336, 411, 539, and 575 (log ϵ, M^{-1} cm^{-1}, 4.3, 5.5, 4.3, and 4.1).

Zn6: ^{1}H NMR (250 MHz, $CDCl_3$) δ 2.49 (s, 12H, Me), 3.13 (t, J = 8.0 Hz, 8H, CH_2-CH_2-COOMe), 3.67 (s, 12H, MeO), 4.30 (t, J = 8.0 Hz, 8H, CH_2-CH_2-COOMe), 7.46−8.45 (m, 8H, aryl-*H*), 10.19 (s, 2H, *meso*-H); ^{13}C NMR (100 MHz, $CDCl_3$) δ 15.6 (Me), 21.9 (CH_2-CH_2-COOMe), 36.9 (CH_2-CH_2-COOMe), 51.7 (MeO), 93.7 (aryl-I), 97.7 (*meso*-H), 118.2 (*meso*-aryl), 129.2, 132.4, 137.5 and 142.0 (aryl-H), 139.0, 141.8, 146.1 and 147.5 (pyrrole), 145.5 (aryl-porph), 173.5 (COOMe); FAB calcd for $C_{52}H_{51}O_8N_4I_2Zn$ 1178.2 [M^+], found 1177.4; λ_{max} (CH_2Cl_2)/nm 338.5, 411.5, 539.5, and 575.5 (log ϵ, M^{-1} cm^{-1}, 3.2, 4.7, 3.3, and 3.0).

Preparation of Ni7. Zn4 (330 mg, 0.29 mmol) was dissolved in $CHCl_3$ (20 mL) and the solution washed with MeOH/TFA (2 × 25 mL, 10%) and H_2O (4 × 100 mL). The organic layer was dried, and $Ni(OAc)_2$·$4H_2O$ (300 mg, 1.2 mmol) and MeOH (0.2 mL) were added. The reaction mixture was refluxed for 24 h, after which it was allowed to cool and filtered to remove the excess of $Ni(OAc)_2$·$4H_2O$. The solution was concentrated and recrystallized by layered addition of MeOH which yielded the title compound (301 mg, 92% yield): IR ν_{max}(KBr)/cm^{-1} 2952 (CH), 1737 (CO); ^{1}H NMR (400 MHz, $CDCl_3$) δ 0.29 (s, 18H, Me_3Si), 2.31 (s, 12H, Me), 2.99 (t, J = 7.9 Hz, 8H, CH_2-CH_2-COOMe), 3.72 (s, 12H, MeO), 4.07 (t, J = 7.9 Hz, 8H, CH_2-CH_2-COOMe), 7.60−7.95 (m, 8H, aryl-*H*), 9.53 (s, 2H, *meso-H*); ^{13}C NMR (100 MHz, $CDCl_3$) δ −0.06 (Me_3Si), 15.6 (Me), 21.4 (CH_2-CH_2-COOMe), 36.4 (CH_2-CH_2-COOMe), 51.7 (Me), 94.7 (C≡C-$SiMe_3$), 96.2 (*meso*-H), 104.8 (C≡C-$SiMe_3$), 116.0 (*meso*-Ar), 122.7 (aryl-C≡C), 127.6, 132.0, 132.9 and 136.0 (aryl-H), 139.2, 139.9, 140.4 and 141.8 (pyrrole), 140.8 (aryl-porph), 173.3 (*C*OOMe); FAB calcd for $C_{62}H_{68}O_8N_4Si_2Ni$ 1112.1 [M^+], found 1111; λ_{max} (CH_2Cl_2)/nm 259, 345, 409, 529, and 565 (log ϵ, M^{-1} cm^{-1}, 4.65, 4.22, 5.44, 4.17, and 4.31). The trimethylsilyl groups were removed according to the general procedure (**Ni4** (301 mg, 0.270 mmol) and TBAF (0.30 mmol) in CH_2Cl_2 (25 mL)), giving **Ni7** as a red powder (246 mg, 0.254 mmol, 94% yield). IR ν_{max}(KBr)/cm^{-1} 3282 (C≡C-*H*), 2950 (CH), 1731.5 (CO); ^{1}H NMR (400 MHz, $CDCl_3$) δ 2.29 (s, 12H, Me), 2.98 (t, J = 7.7 Hz, 8H, CH_2-CH_2-COOMe), 3.18 (s, 2H, C≡C-*H*), 3.71 (s, 12H, MeO), 4.06 (m, 8H, CH_2-CH_2-COOMe), 7.60−8.02 (m, 8H, aryl-*H*), 9.52 (s, 2H, *meso-H*); ^{13}C NMR (100 MHz, $CDCl_3$) δ 15.5 (Me), 21.4 (CH_2-CH_2-COOMe), 36.4 (CH_2-CH_2-COOMe), 51.7 (MeO), 77.8 (C≡C-H), 96.3 (*meso*-H), 83.5 (C≡C-H), 115.8 (*meso*-aryl), 121.6 (aryl-C≡C), 127.7, 132.1, 133.2 and 136.3 (aryl-H), 139.2 139.8, 140.3 and 142.0 (pyrrole), 140.9 (aryl-porph), 173.3 (*C*OOMe); λ_{max} (CH_2Cl_2)/nm 247, 296, 345, 408, 529 and 565 (log ϵ, M^{-1} cm^{-1}, 4.4, 4.1, 4.1, 5.3, 4.1, and 4.2).

Synthesis of Linear Trimer $Zn_3$9. Zn5 (200 mg, 0.174 mmol), **Zn7** (95 mg, 0.096 mmol), $Pd(PPh_3)_4$ (20 mg, 0.017 mmol), and CuI (7 mg, 0.035 mmol) were dissolved in freshly distilled THF (50 mL) and NEt_3 (50 mL). The solution was saturated with Ar (four freeze−thaw cycles) and heated at 85 °C for 24 h, after which the solvent was removed *in vacuo* and the residue chromatographed through SiO_2, eluting first with CH_2Cl_2/$CHCl_3$ (1:0.5) until a first band clearly separated. The elution was continued with CH_2Cl_2/$CHCl_3$ (1:1) to ensure that the column was free of the first band and finally with CH_2Cl_2/$CHCl_3$ (1:2), giving **$Zn_3$8** (220 mg, 84% yield) as a fine red powder: ^{1}H NMR (400 MHz, $CDCl_3$) δ 0.23 (s, 18H, Me_3Si), 2,47, 2.51 and 2.52 (s, 36H, Me), 3.11 (br s, 24H, CH_2-CH_2-COOMe), 3.62, 3.63, 3.64 and 3.65 (s, 36H, MeO), 4.30 (br s, CH_2-CH_2-COOMe), 7.72−8.28 (m, 24H, aryl-*H*), 10.18 (br s, 6H, *meso-H*); λ_{max} (CH_2Cl_2)/nm 260, 334, 411, 540, and 575 (log ϵ, M^{-1} cm^{-1}, 4.7, 4.8, 5.9, 4.7, and 4.4). The TMS groups were removed using the general procedure described earlier (**$Zn_3$8** (125 mg, 0.0415 mmol) and TBAF (0.095 mmol) in CH_2Cl_2(150 mL)), giving in **$Zn_3$9** as a dark red powder (114 mg, 95% yield): ^{1}H NMR (400 MHz, $CDCl_3$) δ 2.46, 2.51 and 2.52 (s, 36H, Me), 3.12 (t, J = 7.8 Hz, 24H, CH_2-CH_2-COOMe), 3.62, 3.62, 3.63 and 3.65 (s, 36H, MeO), 4.30 (t, J = 7.8 Hz, 24H, CH_2-CH_2-

(35) Press, W. H.; Flannery, B. P.; Tenkolsky, S. A.; Vetterling, W. T. *Numerical Recipes in Pascal*; Cambridge University Press: Cambridge, 1989; pp 547−571.

COOMe), 7.71−8.27 (m, 24H, aryl-*H*), 10.19 (s, 6H, *meso-H*); FAB calcd for $C_{164}H_{152}O_{24}N_{12}Zn_3$ 2872 [M^+], found 2872, 1436 [M^{2+}], found 1435; λ_{max} (CH_2Cl_2)/nm 287, 414, 541, 576, and 738 (log ϵ, M^{-1} cm^{-1}, 5.0, 5.9, 4.7, 4.5, and 4.1).

Untemplated Synthesis of $Zn_3$3. $Zn_3$9 (31.0 mg, 0.0108 mmol) was dissolved in CH_2Cl_2 (50 mL, distilled *ex.* CaH_2). CuCl (74.4 mg, freshly prepared) and TMEDA (115 μl, 0.75 mmol) were then added, and the mixture was stirred under dry air for 90 min. The solution was washed with H_2O (3 × 200 mL), the solvent removed, and the residue chromatographed through SiO_2, eluting with CH_2Cl_2/$CHCl_3$ (1:2). **$Zn_3$3** (14 mg, 45% yield) was obtained as a red powder. (See spectroscopic data below.)

Templated Synthesis of $Zn_3$3. $Zn_3$9 (35 mg, 0.0122 mmol) was dissolved in CH_2Cl_2 (50 mL, distilled *ex.* CaH_2), to which **Py_3T** (5 mg, 0.0160 mmol) was added, and the mixture was stirred for 20 min. CuCl (84 mg, freshly prepared) and TMEDA (129 μL, 0.75 mmol) were then added, and the mixture was stirred under dry air for 18 h. The solution was washed with H_2O (2 × 200 mL), MeOH/TFA (50 mL, 10%) was added, and the mixture was allowed to stir for 1 h and finally washed with H_2O (4 × 500 mL). The solvent was removed and the residue chromatographed through SiO_2, eluting with CH_2Cl_2/$CHCl_3$ (1:2), to afford **$H_6$3** (21 mg, 65% yield): IR ν_{max}(KBr)/cm^{-1} 3447 (NH), 2949 (CH), 1736 (CO); ^{1}H NMR (400 MHz, $CDCl_3$) δ 2.41, 2.48 and 2.50 (s, 36H, Me), 3.01 (m, 24H, CH_2-*CH_2*-COOMe), 3.53, 3.54 and 3.55 (s, 36H, MeO), 4.24 (m, 24H, *CH_2*-CH_2-COOMe), 7.73−8.13 (m, 24H, aryl-*H*), 10.11 and 10.13 (s, 6H, *meso-H*); ^{13}C NMR (100 MHz, $CDCl_3$) δ 14.9 (Me), 21.8 (*CH_2*-CH_2-COOMe), 36.8 (CH_2-*CH_2*-COOMe), 51.6 (MeO), 74.4, 81.6 and 90.1 (C*sp*), 96.7 and 96.8 (*meso*-H), 116.7, 117.2 and 117.3 (*meso*-aryl), 121.3, 122.6 and 122.7 (aryl-C*sp*), 128.0, 132.0, 132.1, 132.6, 132.8, 133.2, 135.2 and 135.5 (aryl-H), 136.9, 137.0, 137.1, 140.9, 141.0, 141.2, 141.3, 141.3, 144.7, 144.78 and 144.84 (pyrrole), 142.1 and 142.2 (aryl-porph), 173.3 (*C*O); FAB calcd for $C_{164}H_{156}O_{24}N_{12}$ 2679 [M^+], found 2679, 1340 [MH^{2+}]; λ_{max} (CH_2Cl_2)/nm 298, 335, 408, 507, 541, 575, and 628 (log ϵ, M^{-1} cm^{-1}, 4.4, 4.4, 5.3, 4.1, 3.6, 3.8, and 3.2).

$H_6$3 was metalated using the general procedure to give **$Zn_3$3** in near quantitative yield: ^{1}H NMR (400 MHz, $CDCl_3$) δ 2.36, 2.43 and 2.45 (s, 36H, Me), 2.99 (m, 24H, CH_2-*CH_2*-COOMe), 3.54, 3.55 and 3.56 (s, 36H, MeO), 4.19 (m, 24H, *CH_2*-CH_2-COOMe), 7.71−8.09 (m, 24H, aryl-*H*), 10.06 (*meso-H*); FAB calcd for $C_{164}H_{150}O_{24}N_{12}Zn_3$ 2869 [M^+], found 2868, 1435 [M^{2+} + H]; λ_{max} (CH_2Cl_2)/nm 338, 412, and 541 (log ϵ, M^{-1} cm^{-1}, 4.9, 6.0, and 4.7).

Synthesis of Linear Trimer $NiZn_2$9. In a procedure similar to that employed in the synthesis of **$Zn_3$9** (see above), **Zn5** (200 mg, 0.174 mmol), **Ni7** (105 mg, 0.108 mmol), $Pd(PPh_3)_4$ (20 mg, 0.017 mmol), CuI (7 mg, 0.035 mmol), freshly distilled THF (50 mL), and NEt_3 (50 mL) were used to prepare **$NiZn_2$8** (195 mg, 74% yield): ^{1}H NMR (250 MHz, $CDCl_3$) δ 0.29 and 0.30 (s, 18H, Me_3Si), 2.33, 2.48 and 2.54 (s, 36H, Me), 2.93 (br s, 8H, CH_2-*CH_2*-COOMe of the nickel porphyrin), 3.11 (br s, 16H, CH_2-*CH_2*-COOMe of the Zn porphyrins), 3.65 and 3.65 (s, 36H, MeO), 4.01 (br s, *CH_2*-CH_2-COOMe of the Ni porphyrin), 4.25 (br s, *CH_2*-CH_2-COOMe of the Zn porphyrins), 7.63−8.32 (m, 24H, aryl-*H*), 9.46 (br s, 2H, *meso-H* of the Ni porphyrin), 10.10 (br s, 4H, *meso-H* of the Zn porphyrins). The trimethylsilyl groups were removed using the general procedure described earlier, **$NiZn_2$8** (188 mg, 0.0625 mmol) and TBAF (0.150 mmol) in CH_2Cl_2 (200 mL), to give **$NiZn_2$9** as a red powder (178 mg, 99% yield): ^{1}H NMR (250 MHz, $CDCl_3$) δ 2.24, 2.46 and 2.52 (s, 36H, Me), 2.90 (t, J = 7.8 Hz, 8H, CH_2-*CH_2*-COOMe of the Ni porphyrin), 3.12 (t, J = 7.5 Hz, 16H, CH_2-*CH_2*-COOMe of the Zn porphyrins), 3.65 and 3.71 (s, 36H, MeO), 3.98 (t, J = 7.8 Hz, 8H, *CH_2*-CH_2-COOMe of the Ni porphyrin), 4.30 (br s, 16H, *CH_2*-CH_2-COOMe of the Zn porphyrins), 7.56−8.27 (m, 24H, aryl-*H*), 9.43 (s, 2H, *meso-H* of the Ni porphyrin), 10.17 (s, 4H, *meso-H* in the Zn porphyrins); FAB calcd for $C_{164}H_{153}O_{24}N_{12}Zn_2Ni$ 1433 [MH^{2+}], found 1433.

Templated Synthesis of $NiZn_2$3. In a procedure similar to that employed in the synthesis of **$Zn_3$3** (see above), **$NiZn_2$9** (50 mg, 0.0175 mmol), **Py_3T** (7 mg, 0.0224 mmol), CuCl (120 mg), and TMEDA(180 μL) in CH_2Cl_2 (60 mL) were combined, and the mixture was stirred under dry air for 14 h. The solution was washed with H_2O (2 × 200 mL), and MeOH/TFA (50 mL, 10%) was added with stirring for 20 min. The solution was then washed with H_2O (4 × 500 mL). The solvent was removed and the residue chromatographed through SiO_2, eluting with CH_2Cl_2/$CHCl_3$ (1:1.5), to give **$NiH_4$3** as a fine red powder (36 mg, 75% yield): IR ν_{max}(KBr)/cm^{-1} 3447 (NH), 2948 (CH), 1735 (CO); ^{1}H NMR (250 MHz, $CDCl_3$) δ 2.21, 2.47 and 2.56 (s, 36H, Me), 2.85 (m, 8H, CH_2-*CH_2*-COOMe of the Ni porphyrin), 3.08 (m, 16H, CH_2-*CH_2*-COOMe of the Zn porphyrins), 3.56, 3.60 and 3.62 (s, 36H, MeO), 3.91 (m, 24H, *CH_2*-CCOOMe of the Ni porphyrin), 4.31 (m, 24H, *CH_2*-CH_2-COOMe of the Zn porphyrins), 7.65−8.17 (m, 24H, aryl-*H*), 9.38 (s, 2H, *meso-H* of the Ni porphyrin) and 10.19 (s, 4H, *meso-H* of the Zn porphyrins); ^{13}C NMR (100 MHz, $CDCl_3$) δ 14.97, 15.0 and 15.4 (Me), 21.4 and 21.9 (*CH_2*-CH_2-COOMe), 36.4, 36.89 and 36.92 (CH_2-*CH_2*-COOMe), 51.6 and 51.7 (MeO), 74.5, 81.8, 90.0 and 90.1 (C*sp*), 96.1 and 96.9 (*meso*-H), 116.3, 116.8 and 117.4 (*meso*-aryl), 121.4, 122.7 and 122.9 (aryl-C*sp*), 127.9, 128.0, 131.6, 131.7, 132.1, 132.6, 132.7, 133.4, 136.0 and 136.3 (aryl-H), 137.0, 137.2, 139.2, 139.7, 140.9, 141.0, 141.1, 141.40, 141.43, 144.8 and 145.0 (pyrrol), 141.6, 142.1 and 142.3 (aryl-porph), 173.3, 173.42 and 173.45 (*C*O); FAB calcd for $C_{164}H_{155}O_{24}N_{12}Ni$ 2736.8 [MH^+], found 2738, 1368 [MH^{2+}]. **$NiH_4$3** was metalated using the general procedure to give **$NiZn_2$3** in near quantitative yield. ^{1}H NMR (400 MHz, $CDCl_3$) δ 2.12, 2.36 and 2.45 (s, 36H, Me), 2.72 (m, 8H, CH_2-*CH_2*-COOMe of the Ni porphyrin), 3.01 (m, 16H, CH_2-*CH_2*-COOMe of the Zn porphyrins), 3.49, 3.56 and 3.58 (s, 36H, MeO), 3.83 (m, 8H, *CH_2*-CH_2-COOMe of the Ni porphyrin), 4.21 (m, 16H, *CH_2*-CH_2-COOMe of the Zn porphyrins), 7.61−8.13 (m, 24H, aryl-*H*), 9.29 (*meso-H* of the Ni porphyrin), 10.06 (*meso-H* of the Zn porphyrins); FAB calcd for $C_{164}H_{150}O_{24}N_{12}NiZn_2$ 2862.5 [M^+], found 2862, 1431 [M^{2+}]; λ_{max} (CH_2Cl_2)/nm 238, 294, 336, 410, and 539 (log ϵ M^{-1} cm^{-1} 5.0, 4.9, 4.9, 5.9 and 4.5).

Host Molecule−Oligopyridine 1:1 Complex. The host molecule (*ca.* 10 m) was dissolved in $CHCl_3$ (10 mL), and the oligopyridine (10 mg) was added. The mixture was stirred at room temperature for 30 min and the solution filtered through SiO_2 (1 cm diameter, 10 cm length), eluting with $CHCl_3$, and dried *in vacuo* to afford the complex in near quantitative yield.

$Zn_3$9−Py_3T 1:1 Complex: ^{1}H NMR (400 MHz, $CDCl_3$) δ 1.89 (m, 6H, α-H in **Py_3T**), 2.39, 2.40, 2.42, 2.45 and 2.50 (s, 32H, Me), 2.95 (m, 24H, CH_2-CH_2-COOMe), 3.45, 3.46 and 3.50 (s, 32H, MeO), 4.09 (m, 24H, CH_2-CH_2-COOMe), 5.78 (m, 6H, βH in **Py_3T**), 7.86−8.28 (m, 24H, aryl-H), 9.81, 9.82 and 9.87 (s, 6H, *meso*-H).

$Zn_3$3−Py_3T 1:1 Complex: ^{1}H NMR (400 MHz, $CDCl_3$) δ 1.68 (d, J = 5.5 Hz, 2H, Hα in **Py_3T**), 1.94 (d, J = 6.2 Hz, 4H, Hα′ in **Py_3T**), 2.39, 2.48 and 2.50 (s, 32H, Me), 2.94 (m, 24H, CH_2-CH_2-COOMe), 3.44, 3.45 and 3.46 (s, 32H, MeO), 4.12 (m, 24H, CH_2-CH_2-COOMe), 5.79 (d, J = 6.2 Hz, 4H, Hβ′ in **Py_3T**), 5.83 (d, J = 5.5 Hz, 2H, Hβ′ in **Py_3T**), 7.72, 7.79 and 7.85 (dd, J = 7.8 and 7.8 Hz, 6H, H5 in the aryl groups), 7.85−8.24 (m, 12H, H4 and H6 in the aryl groups), 8.27 and 8.41 (s, H2 of the aryl groups), 9.82 and 9.87 (s, 6H, *meso*-H); λ_{max} (CH_2Cl_2)/nm 339, 422, and 551 (log ϵ, M^{-1} cm^{-1}, 5.1, 6.0 and 4.7).

Acknowledgment. We thank the European Union Human Capital and Mobility Program (A.V.F.) and EPSRC (N.B.) for financial support, the EPSRC Mass Spectrometry Service in Swansea for mass spectra, and Dr. C. M. Müller for valuable advice and discussion.

IC971235N